Available online at www.sciencedirect.com
ScienceDirect
Journal of Power Sources 160 (2006) 1088–1095
JOURNAL OF POWER SOURCES
www.elsevier.com/locate/jpowsour

Electrical test methods for on-line fuel cell ohmic resistance measurement

K.R. Cooper*, M. Smith

Scribner Associates, Inc., 150 E. Connecticut Ave., Southern Pines, NC 28387, USA

Received 23 January 2006; received in revised form 20 February 2006; accepted 24 February 2006
Available online 18 April 2006

Abstract

The principles and trade-offs of four electrical test methods suitable for on-line measurement of the ohmic resistance (R_Ω) of fuel cells is presented: current interrupt, AC resistance, high frequency resistance (HFR), and electrochemical impedance spectroscopy (EIS). The internal resistance of a proton exchange membrane (PEM) fuel cell determined with the current interrupt, HFR and EIS techniques is compared. The influence of the AC amplitude and frequency of the HFR measurement on the observed ohmic resistance is examined, as is the ohmic resistance extracted from the EIS data by modeling the spectra with a transmission line model for porous electrodes. The ohmic resistance of a H_2/O_2 PEM fuel cell determined via the three methods was within 10–30% of each other. The current interrupt technique consistently produced measured cell resistances that exceeded those of the other two techniques. For the HFR technique, the frequency at which the measurement was conducted influenced the measured resistance (i.e., higher frequency providing smaller R_Ω), whereas the AC amplitude did not effect the observed value. The difference in measured ohmic resistance between these techniques exceeds that reasonably accounted for by measurement error. The source of the discrepancy between current interrupt and impedance-based methods is attributed to the difference in the response of a non-uniformly polarized electrode, such as a porous electrode with non-negligible ohmic resistance, to a large perturbation (current interrupt event) as compared to a small perturbation (impedance measurement).

Keywords: Fuel cell; Ohmic resistance; Current interrupt; Impedance; High frequency resistance

1. Introduction

Successful commercialization and acceptance of fuel cell power systems will demand that these products are as durable and reliable as existing technologies. For example, target fuel cell performance requirements for transportation applications are to achieve the same level of durability and reliability of current automotive engines, i.e., 5000 h lifespan (150,000 miles equivalent) and the ability to function over the full range of vehicle operating conditions (−40 °C to 80 °C) [1,2]. For stationary applications, more than 40,000 h of reliable operation in temperatures from −35 °C to 40 °C are required for market acceptance [1]. In order to develop as well as monitor the health of such devices, test methods that are capable of measuring important properties of the fuel cell performance during active service are necessary. To be suitable for implementation in operating systems, these diagnostic methods must be non-intrusive, not impact the performance of the cell, be easily implemented, and the results easily interpreted.

Ohmic resistance (R_Ω) is a key performance driver of fuel cells [3,4]. The three sources of ohmic voltage loss are: (a) resistance to ion migration within the electrolyte, (b) resistance to electron transport within the cell components (electrodes, gas diffusion layer, and flow field/current collectors), and (c) contact resistances. Although the dominate source of ohmic resistance varies with the type of fuel cell, the total internal resistance of a fuel cell (or fuel cell stack) is an important consideration: small amounts of ohmic resistance (on the order of milliohms) have a significant effect on overall efficiency because of the high current densities at which these electrochemical devices generally operate [4]. As a result, it is desirable to measure the resistance of the cells during their development, manufacture, and long-term operation.

This article examines and compares presently available methods for measuring the internal resistance of fuel cells during operation. Because the resistance of the cell is often a complex function of many parameters (e.g., temperature, current density, hydration, etc.) it is desirable to measure the resistance of the

* Corresponding author. Tel.: +1 910 695 8884; fax: +1 910 695 8886.
E-mail address: kevin@scribner.com (K.R. Cooper).

0378-7753/$ – see front matter © 2006 Elsevier B.V. All rights reserved.
doi:10.1016/j.jpowsour.2006.02.086

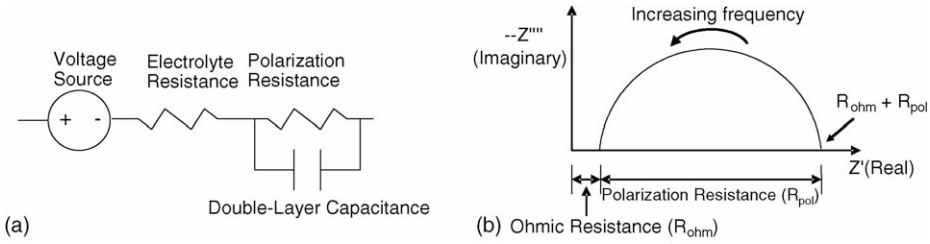

Fig. 1. (a) Simplified, idealized equivalent circuit for a H_2 PEM fuel cell. (b) Nyquist plot of the impedance of the equivalent circuit shown in (a).

cell under operating conditions. Therefore, we focus on methods suitable for on-line, real-time monitoring of functioning cells. The four methods generally used for internal cell resistance measurement are: current interrupt (iR), AC resistance, electrochemical impedance spectroscopy (EIS), and high frequency resistance (HFR). A comparison of these methods follows a discussion of the measurement principle, and the pros and cons of each.

The fuel cell can be modeled by the Randles equivalent circuit shown in Fig. 1(a). This simple model circuit is commonly applied to electrochemical systems in which contact resistance and other effects are small enough to ignore. For simplicity, assume that the polarization resistance of one electrode (say the cathode) is much larger than that of the other electrode (the anode), so that one can legitimately omit circuit elements associated with one of the electrodes (the anode in this example). Polarization resistance is the reaction equivalent, double-layer capacitance is the interfacial capacitance of the cathode, and the ohmic resistance is the resistive component of the fuel cell to be evaluated. The voltage source element is an ideal dc voltage source (zero internal impedance and constant voltage) with a potential equal to the open circuit voltage of the fuel cell. The voltage source element does not affect AC analysis but allows the model to approximate the dc behavior of the fuel cell. Note that the values of these equivalent circuit components are a function of the cell's operating current or voltage, making the fuel cell an electrically non-linear device.

Looking at the equivalent circuit in Fig. 1(a), the double-layer capacitance will exhibit very low impedance at high frequencies, essentially providing a short at the electrochemical interface. At high frequencies only the bulk ionic and electronic ohmic resistance and contact resistances are observed. Cell resistance measurements take advantage of the capacitance of the electrochemical interface which decouples ohmic effects from the activation polarization contributions under some conditions. As described below, this may be implemented several different ways, but all have some traits in common:

- All methods impose a changing electrical condition on the cell.
- All methods measure current and/or voltage waveforms resulting from that change.
- All methods require an accurate voltage measurement directly at the cell terminals using the four-terminal (Kelvin) method.

1.1. Current interrupt method

In this time-domain AC technique, the cell current is very rapidly interrupted and the terminal voltage before and during the interruption measured [5,6]. The current interrupt technique is probably the most widely used method of ohmic drop and ohmic resistance evaluation of electrochemical systems, including batteries [7], corrosion [8,9], and fuel cells [10–12].

The principle of the current interrupter method is shown in Fig. 2. The cell voltage is a combination of the charged anode and cathode potentials less the cumulative resistive potential drop of the electrolyte, electrical conductors, and contact resistances. Thus, in principle, the cell voltage rises nearly instantaneously by the amount of the ohmic potential drop, ΔV (V), upon interruption of the current. The ohmic resistance of the cell R_Ω ($\Omega\,cm^2$) is determined as the quotient of the instantaneous change in voltage and the cell current density i ($A\,cm^{-2}$) just prior to the interrupt event, $R_\Omega = \Delta V/i$.

Advantages of this method include a single data value which is easily interpreted. Furthermore, there is no requirement for additional equipment because the interrupt is brought about by the load. The primary disadvantage of this method is that it imposes a significant perturbation on the cell, if only for a short duration (i.e., tens of micro-seconds). Users of this method are also cautioned that data are degraded when long cell cables are used due to excessive 'ringing' caused by cable inductance; leads should be kept as short as possible to minimize pick up of stray

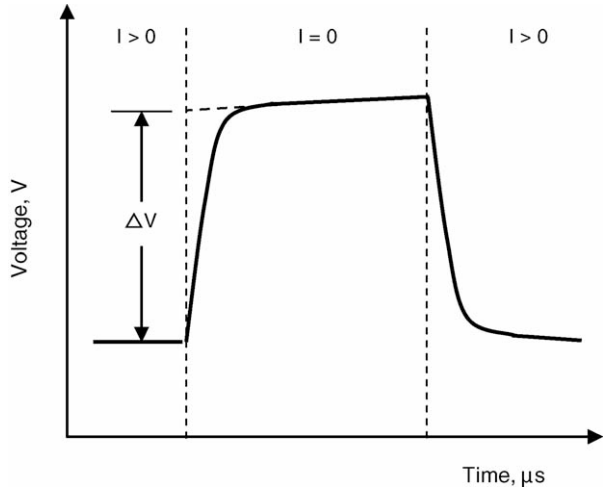

Fig. 2. Idealized voltage waveform during current interrupt event. The ohmic resistance R_Ω ($\Omega\,cm^2$) is the ratio of the instantaneous change in the cell voltage ΔV (V) and the cell current density i ($A\,cm^{-2}$).

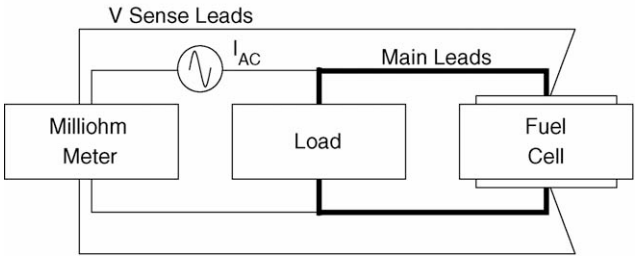

Fig. 3. Resistance measurement of a fuel cell by the AC resistance technique. The impedance measured by the AC milliohm meter is that of the parallel fuel cell–load combination.

capacitances and inductances [7]. Finally, under some circumstances for electrochemical systems with porous electrodes, the interrupter method may overestimate the ohmic voltage change and therefore overestimate the ohmic resistance of the cell. This latter point is discussed further below.

1.2. AC resistance method

This method uses an AC resistance measurement device, such as an external AC milliohm meter, to apply a single, high frequency sine wave (typically ~1 kHz) to the fuel cell under test to measure the total impedance magnitude of the cell and the load in parallel at that frequency. The set-up is shown in Fig. 3. The ohmic resistance of the cell can be extracted after correcting for the impedance of the load.

Like the current interrupt technique, this method provides a single data point. Because the AC perturbation is generally small relative to the dc current, the cell is minimally disturbed electrochemically by the measurement and therefore this method is suitable for interrogation of a functioning cell.

However, accurate results from the AC resistance method require exact gain-phase characterization of the impedance of the load at the operating conditions of the fuel cell during the AC measurement. Knowledge of the complex impedance of the load is required because the milliohm meter measures the zero-phase condition of the parallel fuel cell–load combination, which does not necessarily equal the zero-phase impedance of the cell (i.e., referring to Fig. 3 in this configuration the load has a complex impedance in parallel with the complex impedance of the cell). To accurately determine the high frequency resistance of the fuel cell one should account for the contribution of the impedance of the load to the impedance measured with the AC milliohm meter. As such, one must determine with external frequency analysis equipment the complex impedance of the load at the dc voltage and dc current of interest at the frequency of the AC resistance measurement. The difficulties of this technique stem from the milliohm meter not being intended to measure energy sources under load.

1.3. High frequency resistance method

In the HFR method to determine internal cell resistance, a small AC signal is applied to the electronic load to modulate the dc load current, as illustrated in Fig. 4. The resulting magnitude

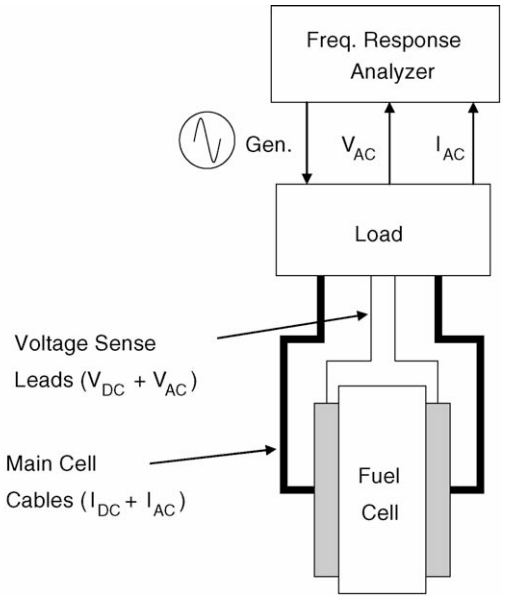

Fig. 4. Equipment set-up for HFR and EIS measurement techniques. The AC signal imposed on the cell is done by modulating the load.

and phase of the AC voltage and current response are measured by a frequency response analyzer. A single, high frequency is used, typically on the order of 1 kHz. This method is actually a subset of the EIS method described below wherein a broad range of frequencies are employed. Of interest is the real component of the impedance (Z' or Re(Z)).

HFR measurement minimally disturbs the cell from its operating condition, both in magnitude and duration, and therefore it is suitable for routine, periodic application during normal fuel cell operation.

The appropriate frequency for an HFR measurement varies with the electrochemical system under study. Selection of the proper frequency is best accomplished by examining the phase difference between the AC current and voltage signals at a range of frequencies. It should ideally be the frequency at which the imaginary component of the impedance is zero (Im(Z) or $Z'' = 0$) and therefore the cell is behaving in a purely resistive manner. In terms of a Nyquist plot, this condition exists when the impedance data cross the real axis (Fig. 1(b)) at high frequency. Typical HFR measurement frequencies range from 1 kHz to 10 kHz. In any case, the same frequency must be used for valid data comparison.

Note that the method for choosing the HFR frequency requires that the test system also have EIS capability. This is generally not a problem because a true frequency response analyzer can measure over a wide range of frequencies, so a test system capable of true HFR measurement will also be capable of performing EIS measurements.

1.4. Electrochemical impedance spectroscopy method

EIS is an extension of the HFR method previously described and differs in two ways. Whereas HFR employs a single frequency and only examines the real component of the impedance, EIS involves imposing the AC perturbation over a broad range of

frequencies – typically 10 kHz to 1 Hz or lower – and monitoring the resulting variations in magnitude and phase of the cell voltage and current in order to determine the complex impedance (Z', Z'', or Z-phase relation) of the electrochemical system being studied. This results in a rich data set from which several parameters may be extracted via equivalent circuit modeling. These parameters include non-electrode ohmic resistance, electrode properties such as ohmic resistance and activation polarization resistance, double-layer capacitance, and transport properties [13–15,16,17].

The real component of the impedance measured using EIS at the frequency used for an HFR measurement should be identical to the resistance obtained using HFR.

2. Experimental

Experiments were conducted on a 23 cm^2 proton exchange membrane (PEM) fuel cell at 50 °C with ambient pressure and humidified reactants (Anode: 1.25× H_2, humidifier at 45 °C; Cathode: 2.0× O_2, humidifier at 45 °C). Fuel and oxidant flow rates were load-controlled such that the indicated stoichiometry was achieved at each of the current densities examined (0.5 A cm^{-2}, 1.0 A cm^{-2}, and 1.5 A cm^{-2}). Testing was performed with a computer-controlled Medusa RD Fuel Cell Test Station (Teledyne Energy Systems, Inc.) with a 50 A/125 W Model 890CL electronic load (Scribner Associates, Inc.) and Model 880 Frequency Response Analyzer (Scribner Associates, Inc.). EIS spectra were modeled with ZView® (Scribner Associates, Inc.).

The main cell cables (i.e., current carrying leads) were 0.57 m (22.5 in.) long and 10.7 mm (0.42 in.) diameter stranded copper. Intertwined conductor cables that were as short as possible were used in order to minimize the inductance generated by rapid voltage or current changes, such as during a current interrupt event or at high frequencies during impedance measurements. Low impedance devices such as fuel cells and batteries require that a four-terminal measurement technique (as illustrated in Fig. 4) be implemented in order to obtain accurate results [18].

The membrane electrode assembly was broken-in prior to performing the series of experiments described below. In addition, before conducting the experiments, the cell was conditioned by repeatedly cycling between 0.7 V and 0.3 V until no change in performance was observed (approximately 10 cycles). Following the conditioning exercise and for each current density, the fuel cell was operated at constant current for 1 h prior to making the resistance measurements. For each operating current density, HFR and current interrupt measurements were obtained for 2 min (at 1 point s^{-1}) which was immediately followed by the impedance spectroscopy experiment. HFR and IR data recorded during the final 60 s were used to determine the mean and standard deviation (σ) of the internal cell resistance at that operating condition (i.e., number of points $N = 60$). In most cases current interrupt and HFR data were acquired simultaneously and it was determined that there was no influence of one measurement technique on the other. That is, both techniques could be applied simultaneously and in real-time without influencing the result of the other.

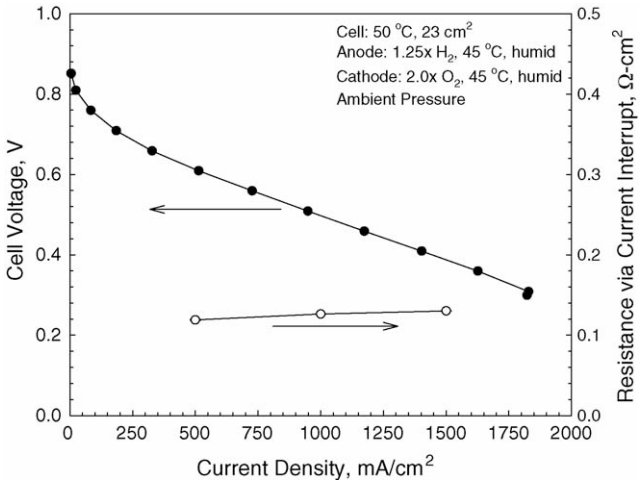

Fig. 5. Polarization curve for the PEM fuel cell used in this work. Cell ohmic resistance determined by current interrupt method was ca. 0.12 Ω cm^2. Test conditions given in figure and in the text.

Specific experimental parameters for the ohmic resistance measurements were as follows. Conservative measurement error estimates are based on the functional specifications of the voltage and current measuring instruments and frequency response analyzer. Additional error associated with equivalent circuit model fit results is included in the EIS error estimate. Error estimates are considered worst-case; typical measurement error will be less than reported here.

2.1. Current interrupt

• Delay time	20 μs
• Error	±(0.3% + 0.2%/ΔV)

2.2. High frequency resistance

• Frequency, ω	1 kHz, 2 kHz, and 5 kHz
• AC current amplitude	2%, 5%, or 10% of dc current
• Error	±3.5%

2.3. Electrochemical impedance spectroscopy

• Frequency range, ω:	10 kHz to 1 Hz
• AC current amplitude:	5% of dc current
• Integration time:	1 s or 10 cycles minimum
• 10 steps per decade	
• Error:	±(3.5% + fitting error[1])

The dc behavior of the cell is shown in Fig. 5.

[1] Estimated errors for fitted parameters are specific for each data set. Estimated errors for results obtained in this work are provided in Table 1.

Table 1
Ohmic resistance (R_Ω) of a H_2/O_2 PEM fuel cell determined by current interrupt and HFR techniques, and modeled EIS data

Current density ($A\,cm^{-2}$)	R_Ω by current interrupt ($m\Omega\,cm^2$) $\mu \pm 1\sigma$ (error)	R_Ω by HFR ($m\Omega\,cm^2$) $\mu \pm 1\sigma$ (3.5% error for all)			R_Ω by EIS + model fit ($m\Omega\,cm^2$) predicted (error)
		1 kHz	2 kHz	5 kHz	
0.5	119.1 ± 0.7 (3.7%)	114.2 ± 0.5	108.8 ± 0.3	100.2 ± 0.2	93.9 (3.9%)
1.0	126.4 ± 0.3 (1.9%)	122.8 ± 0.2	111.7 ± 0.1	112.0 ± 0.1	98.5 (4.0%)
1.5	130.2 ± 0.3 (1.3%)	125.7 ± 0.1	118.0 ± 0.1	115.0 ± 0.4	101.9 (4.3%)

HFR and EIS data acquired with AC signal = 5% of dc current. For current interrupt and HFR techniques the mean ± 1σ are indicated. Error estimates for EIS results are the combined measurement and model fitting errors.

3. Results and discussion

This work examines assessment of the ohmic resistance of PEM fuel cells via techniques suitable for on-line, real-time monitoring, such as might be used for diagnostics and health monitoring. By definition, such techniques must be non-invasive (i.e., not interfere with the normal operation of the fuel cell) nor negatively impact its short- or long-term performance. Furthermore, the results should be easy to interpret. For these reasons, we focus on current interrupt and impedance-based techniques. Of the latter, HFR is a subset of EIS wherein the real component of the impedance, Re(Z), at a fixed, high frequency is assumed to approximate the ohmic resistance of the cell. The ohmic resistance of a H_2/O_2 PEM fuel cell obtained using these three methods are summarized in Table 1.

Note that each method recorded an increase in membrane resistance with increasing current density. Such current-dependent membrane resistance behavior is common among PEM fuel cells. At high current density water molecules associated with migrating protons are dragged from the anode to the cathode at a higher rate than the water can back diffuse from the cathode where water is produced. As such, the membrane on the anode-side of the cell becomes partially dehydrated and its conductivity decreases with the net result being an observed increase in cell ohmic resistance.

Fig. 6 shows the voltage response of the cell during a current interrupt event. Note that the time frame is on the order of tens of micro-seconds (μs). The sudden interruption of the dc current causes inductance in the cell and the cables which is observed as a rapidly decaying, sinusoidal fluctuation in cell voltage during the initial period after the interrupt event (ca. 15 μs). Such 'inductive ringing' is the reason a delay is required before making the ohmic voltage drop (ΔV) measurement. Selection of the duration of the delay period is a balance: it should be as short as possible to minimize the amount of voltage change associated with discharging of the double-layer capacitance of the electrodes but long enough that the post-interrupt voltage measurement occurs after the inductive ringing has sufficiently decayed. Examination of the voltage waveform captured with an oscilloscope during the interrupt event reveals that a 20 μs delay was appropriate for the experimental set-up (cell, cabling, and analytical instrumentation) used in this work.

The ohmic resistance (R_Ω) of the cell, determined by current interrupt (iR), was consistently larger than R_Ω obtained from the HFR or EIS. In addition, the magnitude of R_Ω by HFR decreased with increasing frequency. As such, the deviation between the results obtained via current interrupt and HFR increased with increasing frequency at which the HFR measurement was made. This is shown in Fig. 7 which shows the normalized difference in cell resistance determined via these two techniques at three current densities, i.e. $(R_{HFR} - R_{iR})/R_{iR} \times 100\%$. In all cases, the

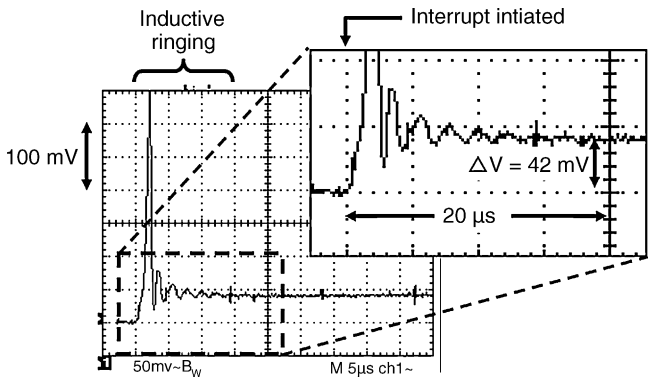

Fig. 6. Oscilloscope trace captured during current interrupt event demonstrating rapid decay in inductive ringing during the first ca. 15 μs after the interrupt. The ohmic voltage drop ΔV was 42 mV (recorded at the 20 μs delay point) and $i = 0.35\,A\,cm^{-2}$ leading to $R_\Omega = 120\,m\Omega\,cm^2$.

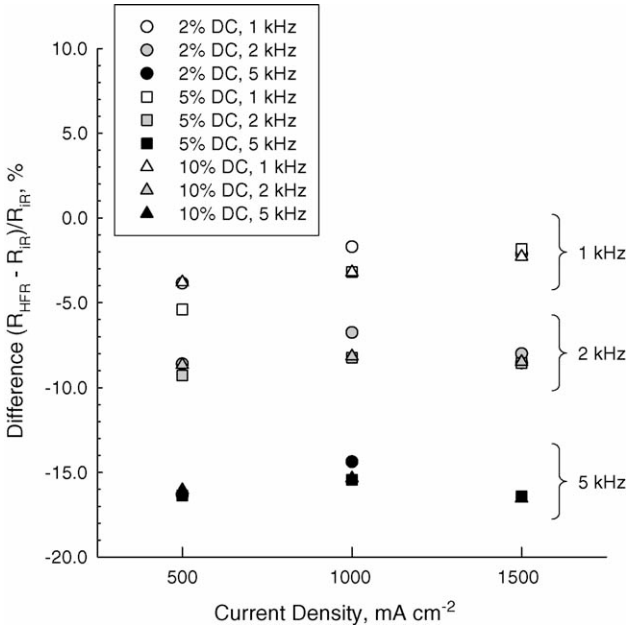

Fig. 7. Normalized difference in cell resistance determined via HFR and current interrupt (iR) techniques at three current densities, i.e. $(R_{HFR} - R_{iR})/R_{iR} \times 100\%$. See text for detailed description. HFR AC amplitude: 2% dc (◯), 5% dc (□), and 10% dc (△).

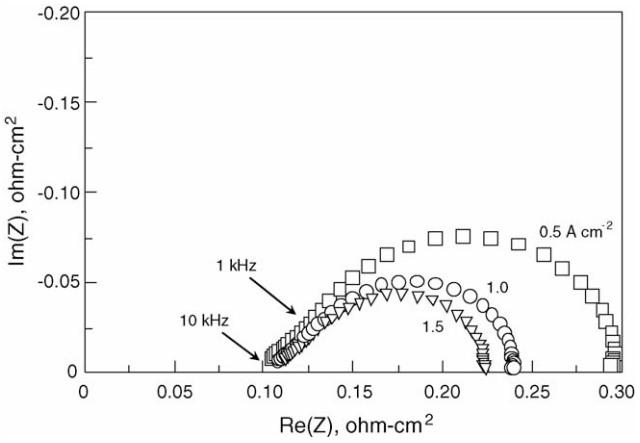

Fig. 8. Complex plane plot showing that with increasing current density, the low frequency resistance decreased, whereas the high frequency resistance increased slightly. R_Ω, estimated by fitting the impedance spectra to the transmission line model (Fig. 9), is summarized in Table 1.

$R_{HFR} < R_{iR}$ and the magnitude of the difference in the results increased with increasing frequency at which the HFR measurement was made.

There was no effect of the AC amplitude on the HFR or EIS results for the range used in this work (i.e., 2–10% of dc current). This is indicated in Fig. 7 by the clustering at each current density of the data acquired at different AC amplitudes. This result is consistent with the fact that: (a) on the low-current end of the test matrix, when the AC signal was 2% of the dc current density ($i_{dc} = 0.5\ A\ cm^{-2}$), the impedance-based techniques were well within the current measuring resolution of the instrument, and (b) the fuel cell was evaluated at current densities at which the V–i response due to the AC perturbation was linear (Fig. 5). The latter point is important because of the requirement to satisfy the linearity criteria for valid impedance measurements [19].

Examination of impedance spectra provides insight into the frequency-dependence of the HFR measurement. It is evident from the impedance spectra shown in Fig. 8 that at 1 kHz, the impedance was not purely resistive, i.e., the imaginary component of the impedance was non-zero, $\mathrm{Im}(Z) < 0$.

To estimate the ohmic resistance of the cell from the EIS measurements, the data were fit to a transmission line model for a porous electrode [14]. The model is shown in Fig. 9. In the model, the measured ohmic resistance of the cell is that portion outside the catalyst layer, namely the sum of the resistance of the membrane to proton transfer ($R_{\Omega,membrane}$) and all other bulk electronic and contact resistances ($R_{\Omega,bulk+contact}$). The transmission line portion of the model represents the catalyst layer where $R_{\Omega,electrode,i}$ and $R_{ct,i}$ are, respectively, the distributed electrolyte resistance and distributed charge-transfer resistance within the reactive layer, and $C_{dl,i}$ is the distributed double-layer capacitance. The usefulness of the transmission line model for characterizing fuel cell electrodes has been demonstrated [14,17]. The focus here is the application of the model for extracting the internal (ohmic) resistance of the cell. For the transmission line model illustrated in Fig. 9, 100 repeating units were used to represent a porous electrode with non-negligible electrolyte resistance. Each repeating unit consisted of a resistor ($R_{\Omega,electrode,i}$) and a parallel resistor–capacitor element ($R_{ct,i}||C_{dl,i}$).

The cell resistance obtained by modeling the EIS data is summarized in Table 1. Only the results for spectra acquired with an AC perturbation current = 5% of the dc current are shown because, as with the HFR measurements, we did not observe an influence of the magnitude of the AC signal on R_Ω (for the range of conditions used in this work). Ohmic resistance values extracted from the model were 20–30% smaller than those measured using the current interrupt technique.

Noting that in the ideal case the bulk (non-electrode) ohmic resistance of the cell is purely resistive in nature, R_Ω does not exhibit an out-of-phase component of impedance (i.e., $\mathrm{Im}(Z) = 0$). By fitting the EIS data we are essentially extrapolating to the $\mathrm{Im}(Z) = 0$ condition in order to estimate R_Ω (this is the value reported in Table 1). Therefore, the discrepancy between R_Ω for the HFR and EIS techniques is due to the fact that in the latter case, R_Ω is the predicted value based on $\mathrm{Im}(Z) = 0$, whereas in the former, R_Ω is taken as the real component of the impedance at the AC frequency at which the measurement was made (in this case, 1 kHz, 2 kHz, or 5 kHz). We can see from the impedance spectra (Fig. 8) that $\mathrm{Im}(Z) < 0$ at all frequencies less than 10 kHz. For this reason, one would expect that R_Ω obtained from an HFR measurement at the frequencies used here would be less than R_Ω estimated from fitting impedance spectra.

For this particular fuel cell operating with moderately humidified reactants, the ohmic resistance by three methods was within 10–30% of each other. Conservative estimates of the measurement error were 1.3–4.3%; error estimates are summarized in Table 1. The difference in measured R_Ω between these techniques exceeds that reasonably accounted for by measurement error. The source of the discrepancy in R_Ω between the current interrupt and impedance-based methods is proposed below.

3.1. Comparison of techniques

The objective here for each of these methods is to determine the electrolyte resistance of the fuel cell. The two techniques

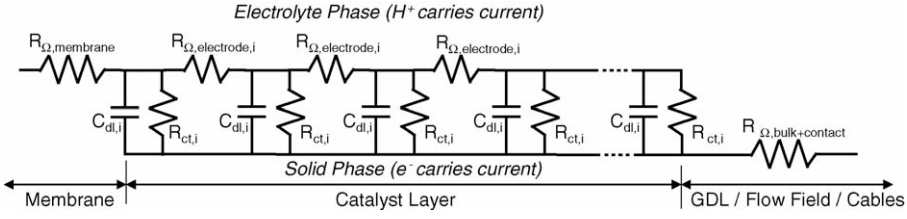

Fig. 9. Equivalent circuit of a H_2/O_2 PEM fuel cell represented by a transmission line model for a porous electrode with non-negligible electrolyte resistance used to model the EIS data. Adapted from [14].

most easily compared are the current interrupt and HFR methods. In practice, the results from these two techniques usually correlate well if the HFR measurement frequency is properly chosen. There are, however, inherent differences in the two methods: the current interrupt method introduces a large perturbation to the fuel cell and looks at its time-domain response, whereas the HFR method applies a small signal and uses the frequency-domain response of the cell. Discrepancies between results obtained from these two methods derive from whether the current distribution present during the current interruption or impedance measurement is the same as the current distribution during standard dc operation of the cell.

In the current interrupt technique, after the interrupt event, the "true" cell voltage is only measured if the current is zero everywhere within the cell and on the surface of the electrode, or, in the case of a porous electrode with a reactive layer of finite thickness, the current is additionally zero within the multi-phase electrode. This condition exists for a uniform potential distribution on the surface of a planar electrode or within a porous electrode [5]. However, if a potential gradient existed within the electrode under the pre-interrupt condition (i.e., $I > 0$), then after the interruption ionic current within the electrolyte and electronic current within the electrode matrix will exist to eliminate the potential gradient. The current present just after the interrupt event will create additional ohmic voltage drop within the cell which will introduce an error in the resistance measurement. That is, the measured ΔV will not equal the true voltage drop due to pure ohmic resistance within cell. This effect has been described and modeled by Lagergren et al. [10].

This artifact is most likely to occur in porous electrodes in which the ionic conductivity of the electrolyte is of the same order of magnitude as the electronic conductivity of the electrode matrix [20]. The relationship between the magnitude of the error of the ohmic potential drop, $\eta_{\Omega,\text{error}}$, and properties of the electrodes is given by Eq. (1).

$$\eta_{\Omega,\text{error}} = \frac{L}{\kappa_{\text{eff,electrolyte}} + \kappa_{\text{eff,electrode}}} i \quad (1)$$

Here, L is the thickness of the catalyst layer, i the current density, and $\kappa_{\text{eff,electrolyte}}$ and $\kappa_{\text{eff,electrode}}$ are the effective conductivities of the ion conducting pore electrolyte and the electron conducting matrix material of the reactive layer, respectively. The magnitude of the ohmic potential drop error is directly proportional to the geometric current density and thickness of the electrode, and inversely proportional to the sum of the electrolyte and electrode conductivities. Note that $\eta_{\Omega,\text{error}}$ approaches zero with increasing conductivity of either charge-carrying phase. Furthermore, the phase with the highest conductivity determines $\eta_{\Omega,\text{error}}$.

For impedance-based methods such as HFR, the electrolyte resistance is determined from the real component of the impedance measured at high frequency. However, total electrolyte resistance may change with current redistribution. Therefore, the AC signal should be small relative to the dc current such that imposition of the AC signal on the cell does not itself significantly influence the current distribution. The resistance measured in this instance will be similar to that experienced under pure dc conditions and the electrolyte resistance determined with the impedance method will be accurate. The fact that cell resistance obtained with the HFR technique was not a function of the AC signal magnitude (at least for the range of conditions used here, i.e., 2–10% dc current) suggests that the imposed perturbation was not large enough to alter the current distribution due to a change in the resistivity of the electrolyte.

We apply Eq. (1) to determine if the above described effect can be attributed to the discrepancy in the ohmic resistance obtained using current interrupt and impedance-based methods. The thickness of the porous electrode and effective conductivity of the pore electrolyte and electrode matrix are unknown for the cell used in this work. However, reasonable bounded estimates for $\eta_{\Omega,\text{error}}$ can be made based on the following assumptions: $L = 25\ \mu\text{m}$, $10\ \text{mS cm}^{-1} < \kappa_{\text{eff,electrolyte}} < 25\ \text{mS cm}^{-1}$, and $50\ \text{mS cm}^{-1} < \kappa_{\text{eff,electrode}} < 1000\ \text{mS cm}^{-1}$. Conductivity values were based on the work of Srinivasan and co-workers [21] and, more recently, Zawodzinski and co-workers [22,23].

Using these bounding values, $\eta_{\Omega,\text{error}}$ is estimated to range from 2 mV to 42 mV for $i = 1\ \text{A cm}^{-2}$, which corresponds to an overestimate of the cell resistance, $R_{\Omega,\text{over}} = 2\text{–}42\ \text{m}\Omega\ \text{cm}^2$. From Table 1, we see that the difference in measured R_Ω between the current interrupt and EIS + fitted scenario was $28\ \text{m}\Omega\ \text{cm}^2$ at $1\ \text{A cm}^{-2}$. Based on this analysis, it is reasonable to conclude that the source of the discrepancy in measured cell resistance between the current interrupt technique and the impedance method was due to an over-estimation of the ohmic potential drop by the former method due to the existence of a rapid potential change after the interrupt on the polarized porous electrode. The source of discrepancy in measured R_Ω is due to the inherent difference in the response of a porous electrode with non-negligible resistance to a large voltage perturbation (as in the current interrupt technique) versus a small perturbation (as in an impedance measurement).

4. Conclusion

Each of the four methods described may be used to determine the ohmic resistance of an operating fuel cell and therefore are suitable for long-term performance and durability testing and diagnostics. However, users of these techniques should be cognizant of differences in these methods in order to properly apply and interpret the results if accurate and useful measurement of cell resistance is to be obtained.

For a H_2/O_2 PEM fuel cell operating with moderately humidified reactants, the ohmic resistance by three methods – current interrupt, high frequency resistance, and electrochemical impedance spectroscopy – was within 10–30% of each other. Conservative estimates of the measurement error were 1.3–4.3%. The difference in measured ohmic resistance between these techniques exceeds that reasonably accounted for by measurement error.

The discrepancy between R_Ω for the HFR and EIS techniques is due to the fact that in the latter case, R_Ω is the predicted value for the condition that $\text{Im}(Z) = 0$, whereas in the former R_Ω is taken as the real component of the impedance at the AC frequency at which the measurement was made.

The cause of the discrepancy between the impedance-based techniques and the current interrupt method is attributed to additional voltage change observed in the interrupt method as a result of a rapid potential change after the interrupt that arises because of the potential distribution within porous electrodes with non-negligible electrolyte resistance. The inherent difference in the response of a porous electrode with non-negligible ohmic resistance to a large perturbation (current interrupt event) as compared to a small perturbation (impedance measurement) is the source of discrepancy in measured R_Ω for these orthogonal measurement techniques.

References

[1] Hydrogen, Fuel Cells & Infrastructure Technologies Program Multi-Year Research, Development and Demonstration Plan, U.S. Department of Energy, vol. 3, 2005, pp. 69–92, available at http://www.eere.energy.gov/hydrogenandfuelcells/mypp/.

[2] H.A. Gasteiger, M.F. Mathias, Proton conducting membrane fuel cells III, in: M. Murthy, T.F. Fuller, J.W. Van Zee, S. Gottesfeld (Eds.), Proceedings of the International Symposium (PV 2002-31), Salt Lake City, UT, 2005, pp. 1–24.

[3] F. Barbir, PEM Fuel Cells: Theory and Practice, Elsevier Academic Press, Burlington, MA, 2005, pp. 39–45.

[4] J. Laraminie, A. Dicks, Fuel Cells Systems Explained, John Wiley & Sons, New York, NY, 2000, pp. 37–50.

[5] J. Newman, J. Electrochem. Soc. 117 (1970) 507–508.

[6] D. Britz, J. Electroanal. Chem. 88 (1978) 309–322.

[7] M. Hayes, A.T. Kuhn, W. Patefield, J. Power Sources 2 (1977/1978) 121–136.

[8] F. Mansfeld, Corrosion 38 (1982) 56.

[9] H.P. Hack, P.J. Moran, J.R. Scully, in: L.L. Scribner, S.R. Taylor (Eds.), The Measurement and Correction of Electrolyte Resistance in Electrochemical Tests—ASTM STP 1056, American Society for Testing and Materials, Philadelphia, PA, 1990, pp. 5–26.

[10] C. Lagergren, G. Lindbergh, D. Simonsson, J. Electrochem. Soc. 142 (1995) 787–797.

[11] C.-G. Lee, H. Nakano, T. Nishina, I. Uchida, S. Kuroe, J. Electrochem. Soc. 145 (1998) 2747–2751.

[12] F.N. Büchi, A. Marek, G.G. Scherer, J. Electrochem. Soc. 142 (1995) 1895–1901.

[13] T.E. Springer, T.A. Zawodzinski, M.S. Wilson, S. Gottesfeld, J. Electrochem. Soc. 143 (1996) 587–599.

[14] R. Makharia, M.F. Mathias, D.R. Baker, J. Electrochem. Soc. 152 (2005) A970–A977.

[15] B. Andreaus, A.J. McEvory, G.G. Scherer, Electrochim. Acta 47 (2002) 2223–2229.

[16] Q. Guo, M. Cayetano, Y. Tsuo, E.S. De Castro, R.E. White, J. Electrochem. Soc. 150 (2003) A1440–A1449.

[17] M.C. Lefebvre, R.B. Martin, P.G. Pickup, Electrochem. Solid-State Lett. 2 (1999) 259–261.

[18] B. Sayers, in: E. Barsoukov, J.R. Macdonald (Eds.), Impedance Spectroscopy—Theory, Experiment, and Applications, Wiley/Interscience, New York, NY, 2005, pp. 170–171.

[19] B. Sayers, in: E. Barsoukov, J.R. Macdonald (Eds.), Impedance Spectroscopy—Theory, Experiment, and Applications, Wiley/Interscience, New York, NY, 2005, pp. 356–357;
A.J. Bard, L. Faulkner, Electrochemical Methods: Fundamentals and Applications, John Wiley & Sons, New York, NY, 2001, pp. 368–388.

[20] R. Pollard, J. Newman, J. Electrochem. Soc. 128 (1981) 503–507.

[21] C. Boyer, S. Gamburzev, O.A. Velez, S. Srinivasan, A.J. Appleby, Electrochim. Acta 43 (1998) 3703.

[22] A.P. Saab, F.H. Garzon, T.A. Zawodzinski, J. Electrochem. Soc. 149 (2002) A1541–A1546.

[23] A.P. Saab, F.H. Garzon, T.A. Zawodzinski, J. Electrochem. Soc. 150 (2003) A214–A218.